Journal of Ceramic Processing Research. Vol. 18, No. 3, pp. 265~273 (2017)

J O U R N A L O F
Ceramic Processing Research

Effect of use dextrin as bio-dispersants on structural and morphological properties of Al_2O_3 ceramic materials

Matias Scherer Lunkes, Fernanda Dias and Jadna Catafesta*
Postgraduate Program in Materials Science and Engineering (PGMAT), University of Caxias do Sul (UCS), Caxias do Sul, Brazil

Polysaccharides are commonly used as binders in metal oxide colloidal processing. However, if the macromolecular chains are able to adsorb on ceramic particles surface, the suspension deflocculating properties are also favored. This paper investigated the use of dextrin as a bio-dispersant on structural and morphological properties of Al_2O_3 materials. The interaction mechanism between dextrin and Al_2O_3 surface and the additive efficiency of producing less agglomerated systems were discussed. The suspensions behavior was pH-dependent, being the pH 6 the best condition for obtaining more compact systems in dextrin presence. The first monolayer saturation of the Al_2O_3 active sites occurred at 1.5 wt. % of dextrin and a second adsorption layer started above this additive concentration. The highest percentage of densification was 96.25% for the suspension containing 30 vol. % solids and 1 wt. % dextrin. The presence of dextrin also influenced the microstructure of the systems, providing a better bridging between Al_2O_3 particles. The use of dextrin at low dosages proved to be efficient in the stabilization of aqueous alumina suspensions.

Key words: Dextrin, α-Al_2O_3, Dispersant, Adsorption, Ceramic suspension.

Introduction

Alumina (Al_2O_3) is a high performance ceramic material with a wide variety of applications as cutting tools, dies or prosthesis components due to their excellent flexural strength, fracture toughness, and wear resistance [1, 2]. The correlation between dispersion and final product quality has established for the colloidal processing of oxide suspensions [2-4]. In aqueous colloidal processing of Al_2O_3 powders, control of the suspension properties is usually achieved by (i) protonation or deprotonation of the particles surface hydroxyl (-OH) groups, thereby creating a surface charge; (ii) adjustment of the ionic strength or (iii) addition of specific adsorbing organic or inorganic oligo- or polyelectrolyte's [5]. Such stabilizing agents used in the preparation of highly concentrated alumina suspensions include organic [6-8], natural molecules [9, 10] and polymers [11]. These additives adsorb onto the Al_2O_3 surface and form an organic layer around the particles, which improves steric repulsion [12-14]. Additionally, the hydrophilic groups of these stabilizers (carboxylate, sulphonate or sulphate anions, ammonium cations and non-ionic) can change the isoelectric point of the powder surface and interact with the functional groups on the Al_2O_3 phase, thus increasing its binding strength with the polymer [15].

The pyrolysis products of traditional additives results in gasses that cause unwanted cracks and shape distortion in pre-sintered parts. Besides that, carbonaceous residues are not always completely removed and can contaminate microstructures [16]. Water-soluble additives have been chosen as an alternative to these organic chemicals, contributing to a safely evaporation with minimum cracks and microstructure contamination [17]. For this purpose, the additive should enable slurry consolidation to the high powder-packing densities that are needed to minimize shrinkage during drying, rebinding, and sintering [18]. It is also necessary the production of materials with a high degree of plasticity during plastic molding and shape-forming operations [19]. Crack-free green bodies at low concentrations are required for a clean pyrolysis [17].

The literature indicates that saccharides and polysaccharides are promising additives that meet the above demand [17, 19-22]. One of the most common in the market is dextrin, which derived from the acid-catalyzed hydrolysis and/or thermolysis (dextrinization) of granular starch. Dextrins are non-ionic D-glucose polymers of different molecular weight. They are composed of five to several thousand D-glucose units. Dextrins are branched polysaccharides with 1-4, as well as 1-6 glucosidic linkages, that have predominantly higher molecular weight [20, 23, 24]. Water-soluble non-ionic polymeric additives commonly used as binders in metal oxide colloidal processing. Binders confer strength to the green bodies and generally interact with oxide powder surfaces through hydrogen bonding [25]. When the macromolecule is able to adsorb on the ceramic particles surface, however, it can promote sufficient

*Corresponding author:
Tel : +55 (54) 32182088
E-mail: jcatafes@ucs.br

electrostatic repulsive forces to obtain a good state of dispersion [26]. The suspension deflocculating properties are favored by polymer adsorption [20, 27]. At the same time, the not adsorbed (or free) polymer hydroxyl groups in solution contribute to the particles bridging, providing a well cross-linked network [28]. If the macromolecule is capable of forming a strong gelled ceramic, there is no need of adding any external binding agent [29]. The use of a polymer additive that can contribute with dispersing and binding is an attractive solution [30].

Sikora et al. (2002) used dextrin as plasticizers for the aqueous colloidal processing of alumina [17]. They showed that dextrin's with 6450 and 15,000 Daltons were the most efficient from the standpoint of cost and rheological performance. Safinajafabadi and co-workers [20] studied the use of different saccharides in the stabilization of ZTA composites. The lowest sediment height noted for the sample with dextrin when compared with maltose and glucose. This result is a reflection of the larger particle formed, since the larger is the particle size, the faster it settles. The densification rate, as well as mechanical properties, are improved with dextrin [20]. This paper aims to investigate the use of dextrin as a bio-dispersant on structural and morphological properties of Al_2O_3 ceramic materials. We focused on the evaluate efficiency of this highly soluble polysaccharide for the production of less agglomerated Al_2O_3 materials. The knowledge of the interaction mechanism between the dispersant and the ceramic surface may contribute to improve the homogeneous dispersion of the powder [18]. Additionally, the amount of adsorbed dextrin on Al_2O_3 surface related to microstructure and density of green and sintered samples.

Materials

Commercially available α-Al_2O_3 powder (99.8% of purity, diameters of D50 = 0.4 μm and D90 = 2.1 μm and surface area of 7.49 m^2/g) was purchased from Alcoa, Brazil. Dextrin (Amidex 182®) purchased from Ingredion, Brazil. Sodium hydroxide (NaOH) (ACS, 97% of purity) and hydrochloric acid (ACS) purchased from Vetec Chemical, Brazil.

Methods

Settling behavior

Aqueous suspensions of α-$A1_2O_3$ underwent gravity sedimentation in order to investigate the pH condition and the optimum dosage of dextrin capable of maximizing powder compaction. The suspensions were prepared by mixing Al_2O_3 powder and deionized water at room temperature, followed by ball mill homogenization for 24 hrs. 24 suspensions were prepared from four different dextrin concentrations (0 wt.%; 1 wt.%; 2.5 wt.% and 5 wt.% based on alumina mass) and six different pH values (6-11). Each suspension contained 10 vol.% of alumina. Gravity settling monitored as a function of time for 7 days in 50 ml graduated cylinders (Pyrex glass).

Determination of the dextrin amount adsorbed on Al_2O_3 surface

The adsorption of dextrin onto alumina particles quantitatively determined by UV-Vis spectroscopy. A UV-Vis Spectrophotometer (Thermo Scientific Evolution 60) used to measure the concentration of the supernatant dispersant resulting from the separation of the particles. A calibration curve constructed from a stock aqueous solution of dextrin with 3000 mg/L concentration. The pH of the standard solution adjusted to pH 6 with HCl 1 mol/L. The absorbance readings were taken at 280 nm (characteristic wavelength found for dextrin) [31]. An alumina suspension containing 10 vol. % solids was prepared at pH 6 and kept under stirring for 24 hrs in a ball mill (200 rpm). After this period, diluted aliquots of the dextrin stock solution added to the alumina suspension and homogenized for 24 hrs. The systems were ultracentrifuge for 20 min at 15,000 rpm. An aliquot of the supernatant carefully collected and analyzed for non-adsorbed dextrin.

Structural and morphology of Al_2O_3 ceramic materials

Density measurements were performed either by immersion technique in Hg or by using the Archimedes principle. Aqueous alumina suspensions were prepared at high solids loadings (10 vol.%, 20 vol.%, 30 vol.%, 40 vol.%) and ball-milled for 24 hrs at 200 rpm. Solutions containing 0 wt.%; 1 wt.%, 2.5 wt.% and 5 wt. % (based on alumina mass) of dextrin added to each alumina suspension and the systems homogenized for 24 hrs. The specimens were molded in a silicone mold, conditioned at 20 °C and oven dried at 110 °C for 24 hrs to remove residual moisture. Then, the specimens cooled in a desiccator and weighed. The so-obtained green bodies pre-sintered at 1000 °C, according to the heating profile shown in Table 1. This step enables the body's consolidation and the burning out of the organic matter. The pre-sintered bodies then sintered according to the schedule adopted in Table 2. For the green and pre-sintered bodies, the density was measured by Hg immersion since dextrin is soluble in water [32]. After sintering process, the density of the specimens were determined using the Archimedes principle [33].

Microstructural analysis of green and sintered samples carried out using a Shimadzu SSX-550 scanning electron microscopy (SEM). The samples were previously polished using sanding and diamond pastes with different particle sizes (30, 15, 9, 3 and 1 μm). All samples were sputter coated with gold before imaging. For the grain boundary surfaces observation, a thermal attack on the sintered samples was employed according to the profile shown in Table 3 [34].

Table 1. Heating profile employed in dextrin removal and pre-sintering of samples.

Inicial temperature (ºC)	Final temperature (ºC)	Heating rate (ºC/min)	Time (min)
25	275	10	
	275		10
275	320	1.5	
	320		60
320	550	1.5	
550	1000	10	
	1000		60

Table 2. Heating profile used in the sintering of samples.

Inicial temperature (ºC)	Final temperature (ºC)	Heating rate (ºC/min)	Time (min)
25	1600	10	
	1600		120

Table 3. Heating profile for the grain boundary reveal in sintered samples.

Inicial temperature (ºC)	Final temperature (ºC)	Heating rate (ºC/min)	Time (min)
25	1450	10	
	1450		60

Results and Discussion

Settling behavior

The settling behavior of high solids ceramic suspensions been used to provide some indication of dispersion stability [20, 35]. Slurries with well-dispersed particles result in lower settling rate, better stability and enhanced compact sediment bed [36]. Thus, the existence of floc structures in the dispersion state will lead to a loosely packed sediment of low density. Besides influenced by particle density, shape and size distribution, settling densities are also dependent on the powder loading and the aspect ratio of the container. The qualitative precipitation analysis of Al_2O_3 suspensions was performed by separate the effects of competitive surface adsorption between solvent and stabilizing agent, since both additives can have an effect on dispersion state floc structure and hence final sediment density visualizing the sediment-supernatant interface as a function of the settling time. The sediment-supernatant interface represents the separation between the solid sediment (Al_2O_3 particles and adsorbed dextrin) and the clarified liquid (deionized water and non-adsorbed dextrin). The higher the sediment height better is the dispersion. If the suspension settled, it denoted an unstable suspension [19, 37]. The initial height of all suspensions in the cylinders was 132 mm.

The pH of the suspension directly influences the dextrin conformation, which may or may not favor thealumina particles compaction [38]. There is a good correlation between the pH of optimum coprecipitation and the isoelectric points (IEP) of alumina (near pH 9) and dextrin (around pH 4) [39]. The alumina surface positively charged below IEP and negatively charged above the IEP. At pH < 9, alumina particles display a positive zeta potential due to the surface protonation of Al-OH groups to form $Al\text{-}OH^{+2}$ groups. At pH > 9, Al_2O_3 particles display a negative zeta potential due to the surface deprotonation of Al-OH groups to form $Al\text{-}O^{-}$ groups [22, 40]. The repulsion of particles reduced near IEP. Thus aggregation and rapid settling are favored by attractive van der Waals forces [12, 37].

Dextrin adsorption on metal oxides was found to be pH dependent [41]. Zeta potential measurements on dextrin colloids have revealed a negative charge above pH 3.5. The conformation of the adsorbing macromolecules more extended with significant ionization [13, 42]. Thus, the polymer adsorption layer on the solid particle surface is thicker and leads to a more effective electrostatic stabilization of colloidal suspension [42-44]. A feasible interaction was reported under the conditions where mineral surface and dextrin were oppositely charged [45]. Maximum adsorption of dextrin will occur around the pH at which the mineral surface is highly hydroxylase [45, 46]. Protons of dextrin hydroxyls will be easily polarized/ionized, and metal hydroxyl sites will act as scavengers, neutralizing protons.

Fig. 1 shows the behavior of the sediment-supernatant interface of the suspensions as a function of dextrin content and time for different pH values. Suspensions produced at pH 6 containing 0 wt. % and 1wt. % dextrin were stable on the first two days of analysis. No interface for these systems identified in this period. For the other pH values, the sediment-supernatant interface directly detected from the first day of the test. In the absence of any dispersant, the highest interface heights observed for systems prepared at pHs 9 and 10. For being close to their isoelectric point, the Al_2O_3 particles agglomerated rapidly and disorderly, leading to a lower final compaction [47]. Near IEP, attractive interaction between particles is not countered and the suspension achieves its highest flocculated state [37, 48, 49].

The pH 6 was the best condition for obtaining compact pure Al_2O_3 suspensions. For pH values different from 6, the addition of 1 wt. % dextrin seems to have contributed to the opening of the sediment structure, making it less dense. Agglomerated Al_2O_3 particles probably fell under gravity to loosely packed sediments and larger sedimentation heights [3]. For suspensions prepared at pH 6, containing 2.5 wt. % and 5 wt. % dextrin, the additive content increase caused the interface height reduction. This indicates that a more consolidated particulate structure formed. The optimum dispersant concentration is the one that

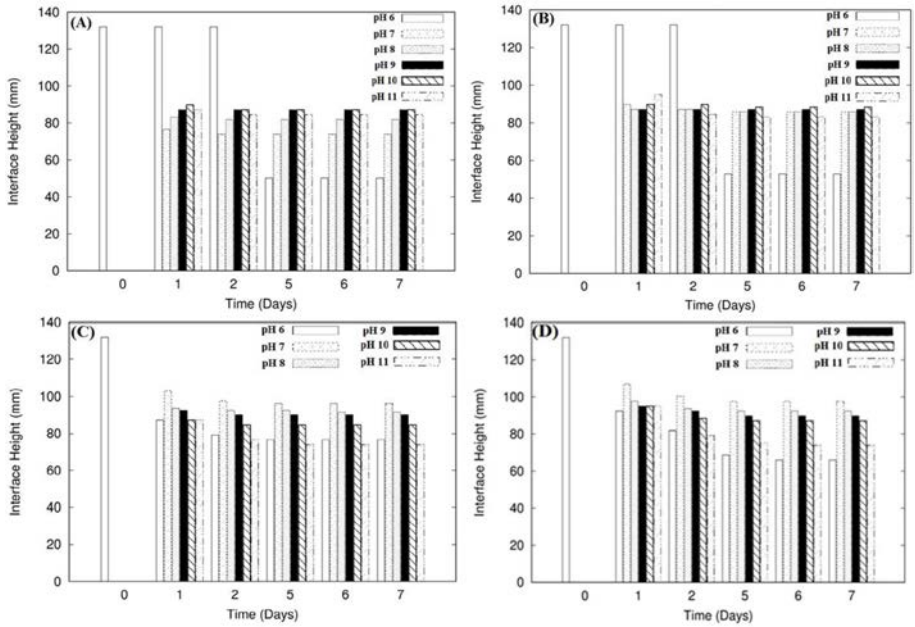

Fig. 1. Sediment heights for suspensions prepared with 0 wt. % (A), 1 wt. % (B), 2.5 wt. % (C) and 5.0 wt. % (D) dextrin as a function of time for different pH values.

provides the lowest sediment height due to an effective particle packing [3, 23, 37, 42].

Too much or too little polymer results in flocculated suspensions with low-density cakes. Low polymer contents produce an incomplete coating of the particles and thus an agglomerated suspension. The excess polymer in the system causes depletion flocculation and loss of stability [13, 46]. When the interactions between dispersant and particle become less efficient, agglomeration will be the only mechanism by which the total free energy of the system can be minimized [35].

The highest interface height for systems containing 2.5 wt. % and 5 wt. % dextrin was observed at pH 7, an intermediate value between the isoelectric points of alumina and dextrin. For pH 8-10 range, higher levels of dextrin resulted in a higher interface height. For pH 11, however, the addition of 2.5 wt. % and 5 wt. % dextrin caused the interface height decrease. This reduction may be related to two factors: shift of the suspension isoelectric point to a pH value distant from 11 or lubricant action of dextrin between Al_2O_3 particles [48]. For the suspensions prepared at pH 6 containing 0 wt. % and 1 wt. % dextrin, a cloudy supernatant was observed on the fifth day. A turbid supernatant, a slow sedimentation and a higher sediment density characterize a dispersed suspension [19, 50, 51]. For the other suspensions, in contrast, the supernatant was transparent regardless of the dextrin content, attesting the sedimentation of Al_2O_3 particles [23, 42]. The pH 6 was chosen as the better condition for particle compaction and sintering.

Determination of the dextrin amount adsorbed on Al_2O_3 surface

UV-Vis spectroscopy analysis performed to quantify the amount of dextrin adsorbed on Al_2O_3 particles surface. Fig. 2 shows the calibration curve obtained for the standard dextrin solution. Fig. 3 shows the amount of dextrin adsorbed (mg/g) on Al_2O_3 as a function of the initial content of dispersant incorporated into the suspension. Dextrin concentrations corresponding to 0.5 wt.%, 1 wt.%, 1.5 wt.%, 2.5 wt.% and 5 wt.% were initially added to the alumina suspensions. The results presented in Fig. 3 were corroborated by thermogravimetric analyzes of alumina samples containing the same incorporated dextrin contents.

It can see that an equilibrium of the adsorbed concentration rate occurs near 1.5 wt. % of dextrin initial content. Then a sharp increase of the adsorbed amount observed for dextrin initial concentrations of 2.5 wt. % and 5 wt. %. It seems that a saturation phenomenon has taken place [52]. Probably, the saturation of the Al_2O_3 active sites occurred through the formation of a dextrin-adsorbed monolayer at the concentration of 1.5 wt. % [35, 40, 43, 53]. For dextrin contents higher than 1.5 wt.%, the results indicate the formation of a second adsorption layer [54].

Thus, the first adsorbed layer in the system corresponds to dextrin concentrations up to 1.5 wt. %. The interaction between alumina and polysaccharides at this first monolayer can be viewed as a Lewis acid-base reaction occurring at the particles surface [19, 20, 22, 41, 55-57]. Polysaccharides have considered adsorbing on mineral surfaces through hydrogen bonds. However, experimental evidences for chemical complexation

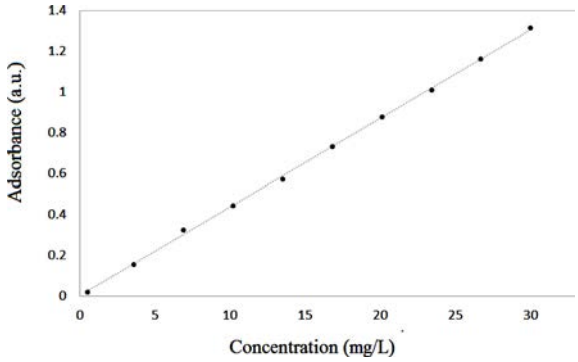

Fig. 2. Calibration curve for the standard dextrin solution.

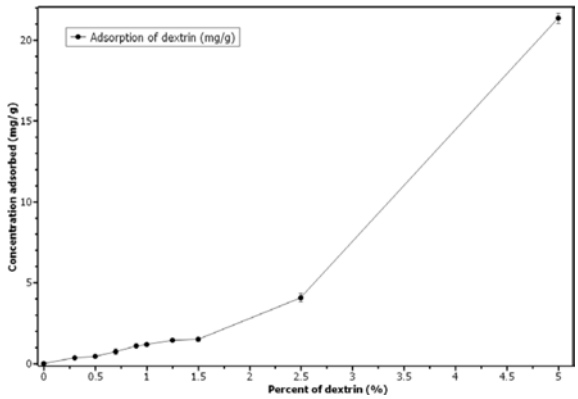

Fig. 3. Adsorbed concentration (mg/g) of dextrin on Al_2O_3 particles as a function of the initial dispersant content.

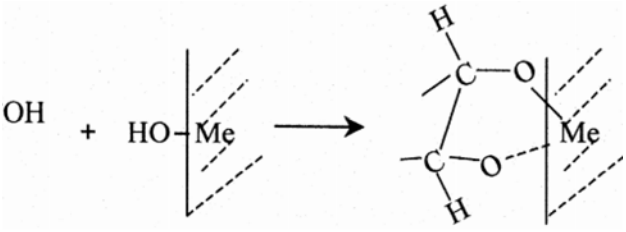

Fig. 4. Formation of the five-membered polysaccharide-metal ring complexes on mineral surfaces.

increasingly reported [40, 45, 58]. The interactions between metal-hydroxylase species and dextrin can result in the formation of a five-membered polysaccharide–metal ring complexes on mineral surfaces (Fig. 4) [22]. The -OH groups corresponding to C-2 and C-3 of the dextrin molecule are in a *cis*-conformation (both on the same side of the monomer ring) and can participate in these complexation reactions [8]. The extent of the acid/base interaction probably determines whether the adsorption is through hydrogen bonding or through chemical complexation. For weak acid/base interactions, only hydrogen bonds may formed. For strong acid/base interactions, it may gradually change to a chemical complexation [22].

The formation of an organic adlayer of dispersants around the ceramic particles produces a steric barrier which prevents agglomeration [3]. The formation of a second adsorption layer, attributed to dextrin concentrations above 1.5% may related to dextrin-dextrin interaction. Due to the saturation of the sites on Al_2O_3 surface, the active groups in dextrin molecule started interacting with itself in the liquid medium [59]. Little known regarding the dynamics of polysaccharides in aqueous suspensions of concentrated oxide particles. Although chromatography studies clearly indicate that polysaccharides sorb on alumina, little is known about the conformation of sorbed polysaccharides or the structure of the solution phase at particle-particle interfaces [13, 42, 60].

Structural and morphology of Al_2O_3 ceramic materials

The variation in density of green alumina compacts with incremental dextrin addition shown in Fig. 5. A stable and well-dispersed colloidal suspension facilitates high packing density in the green body [43, 44]. Uniform green density facilitates homogeneous microstructure of the ceramic component during sintering and thus improves the mechanical properties [44, 61]. Green density increased with increasing solid loading of the suspensions, a key requirement to direct consolidate ceramic slurries [36, 50, 55, 62]. The highest densification levels observed for systems containing 30 vol. % and 40 vol. % Al_2O_3 powder. An increasing number of solids in suspension allows for their mutual approach and prevents segregation phenomena, contributing to a higher density. On the other hand, suspensions with lower solids content form weak aggregates with large pores/voids, leading to lower density values [35].

For 30 vol. % suspension, the green density gradually increased with increasing in dextrin content up to a maximum value and then started decreasing. The dispersant content that resulted in maximum green density can be referred to as optimum composition [6, 10]. A 2.5 wt. % dextrin content led to the highest values of green density for both 30 vol. % and 40 vol. % solids systems. This behavior can be attributed to an inter-particle bridging and cohesion of particles in the presence of the dispersant [57, 63]. A denser packing structure is ensured when a maximum adsorption is attained, indicating full surface coverage of the particles [43]. In contrast, the decrease in density beyond the saturation adsorption level can be related to excess dispersant in the inter-particle spaces, leading to segregation and reduction of compactness [10, 44, 46, 62]. The presence of excess dispersant results in higher shear that limits the flow characteristics of powder mass and lower the packing efficiency [63].

Fig. 6 shows the density results obtained for the pre-sintered bodies. The pre-sintering objective is to remove the organic medium that supports the sample in the green state. In this process, the alumina particles begin to form grains and acquire resistance without the additive presence [34]. It can observed that the pre-sintered density values are rather low. Probably, the organic

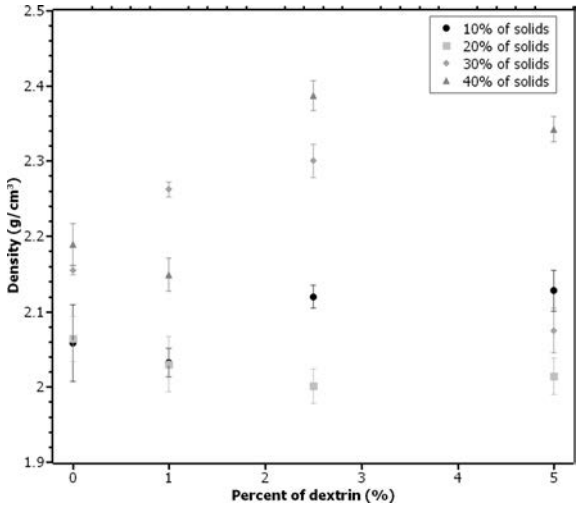

Fig. 5. Green densities of the alumina compacts as a function of the dextrin content and the suspensions solids amount.

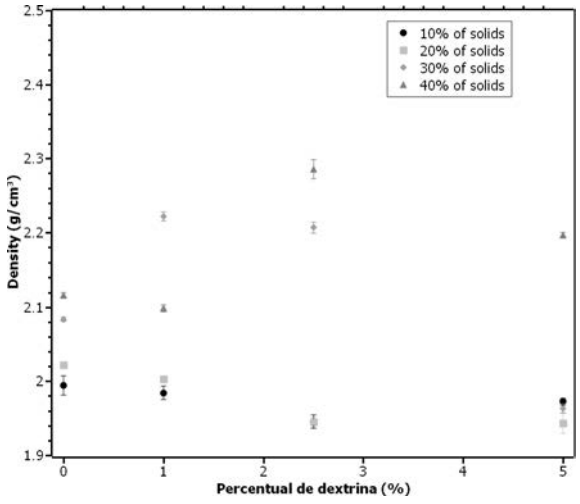

Fig. 6. Pre-sintered densities of the alumina compacts as a function of the dextrin content and the systems solids amount.

additive replaced by air between alumina particles. The entrapped air tends to form bubbles, which in turn, create microdefect's in the bodies [36, 64].

Fig. 7 reports data about sintered densities. Higher values of density obtained because of time and elevated temperature at which the samples submitted. One of the reasons for the increased densification is the

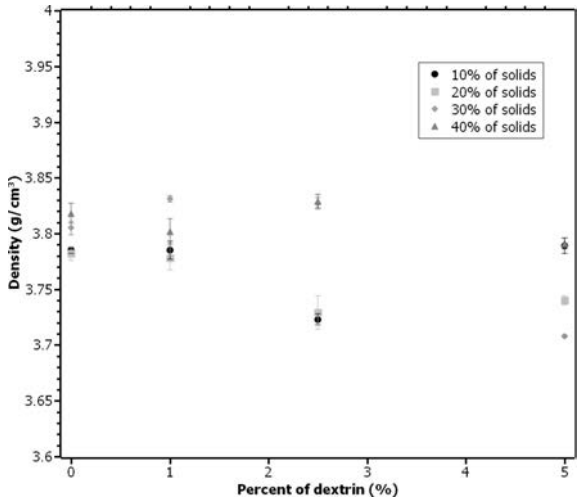

Fig. 7. Sintered densities of the alumina compacts as a function of the dextrin content and the systems solids amount.

Table 4. Densification percentage of the samples in relation to theoretical density.

Dextrin (wt%)	30 vol%solids	40 vol%solids
0	95.60	95.92
1.0	96.25	95.52
2.5	96.15	96.20
5.0	93.16	95.25

formation of additional nucleating sites derived from the dispersant thermal decomposition [63]. The sintered densities followed the same trend observed for the greens, indicating that particle packing influences the densification behavior. Defects or poor particle packing that occur during the forming process, remain throughout the thermal sintering cycle [36, 43, 61, 65]. The highest densities observed for sintered bodies prepared from 30 vol. % and 40 vol. % solid suspensions containing 1 wt. % and 2.5 wt. % dextrin, respectively.

For 2.5 wt. % dextrin concentration, these samples showed very close density values. However, the highest percentage of densification was 96.25% (in relation to the alumina theoretical density) for the sample containing 30 vol. % solids and 1 wt. % dextrin. Table 4 shows the mean values obtained for the densification percentage of the samples in relation to the theoretical density. The densities obtained for the green and

Table 5. Green and sintered densities for samples containing 30vol. % and 40vol. % solids.

Green bodies					Sintered bodies				
Dextrin (wt %)	30vol% (g/cm^3)		40vol% (g/cm^3)		Dextrin (wt %)	30vol% (g/cm^3)		40vol% (g/cm^3)	
0	2.16	± 0.01	2.19	± 0.03	0	3.81	± 0.02	3.82	± 0.02
1.0	2.26	± 0.01	2.15	± 0.02	1.0	3.83	± 0.01	3.80	± 0.02
2.5	2.30	± 0.02	2.39	± 0.02	2.5	3.83	± 0.02	3.83	± 0.01
5.0	2.08	± 0.03	2.34	± 0.02	5.0	3.71	± 0.01	3.79	± 0.01

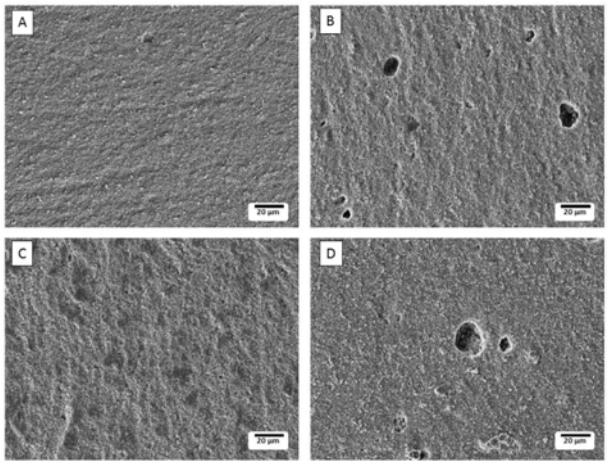

Fig. 8. SEM (500x) of the pre-sintered samples containing 30 vol.% solids and 0 wt.% (A), 1 wt.% (B), 2.5 wt.% (C) and 5 wt.% (D) dextrin.

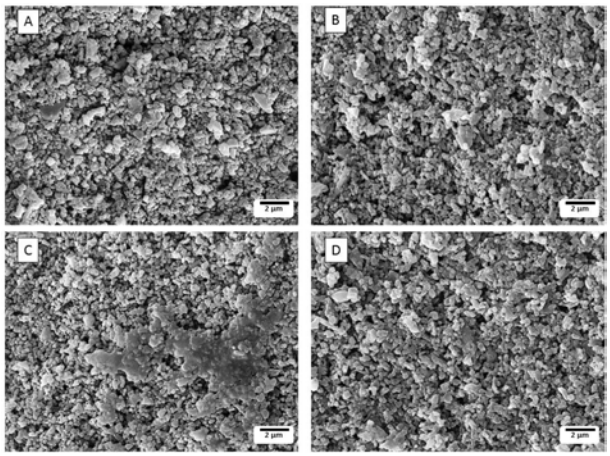

Fig. 9. SEM (5000x) of the pre-sintered samples containing 30 vol.% solids and 0 wt.% (A), 1 wt.% (B), 2.5 wt.% (C) and 5 wt.% (D) dextrin.

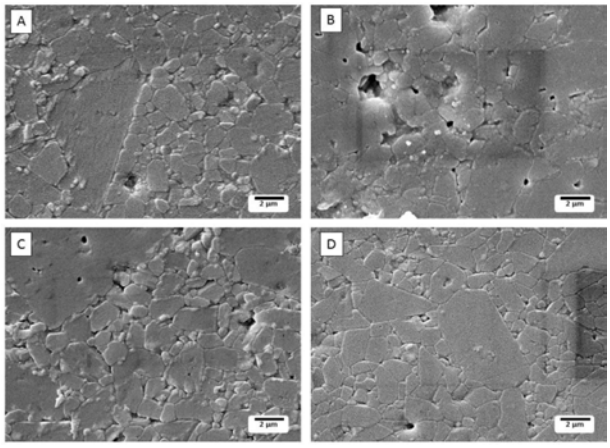

Fig. 10. SEM micrographs (5000x) of the sintered samples containing 30vol.% solids and 0 wt.% (A), 1 wt.% (B), 2.5 wt.% (C) and 5 wt.% (D) dextrin.

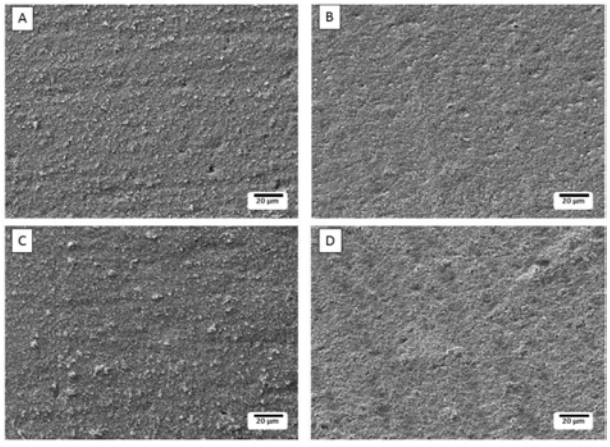

Fig. 11. SEM (500x) of the pre-sintered samples containing 40 vol.% solids and 0 wt.% (A), 1 wt.% (B), 2.5 wt.% (C) and 5 wt.% (D) dextrin.

sintered bodies summarized in Table 5.

The mechanical properties of ceramic materials greatly influenced by their microstructure [66]. One of the challenges of powder technology is to control densification during sintering. So that a sintered body with minimum porosity can be obtained [67]. SEM performed to check the compaction and density variation of pre-sintered and sintered bodies with 30 vol. % and 40 vol. % of alumina particles. The images carried out at 500x and 5000x magnifications. Figs. 8 and 9 show the microstructures of the pre-sintered samples containing 30 vol. % solids and 0, 1, 2.5 and 5 wt. % of dextrin.

Fig. 8 clearly shows the presence of pores in the samples containing 1 wt. % and 5 wt. % dextrin, probably due to entrapped air bubbles in the compacted structure. The presence of these bubbles hinders compaction and directly affects the samples densities. A vacuum system could have used in the green bodies molding process; however, an incorrect power could cause liquid medium sublimation and, consequently, new bubbles formation. Some particle junctions from the thermal heating could be discerned [68]. For system contains 2.5 wt.% dextrin, it seems that some alumina particles are surrounded by a polymer network [69].

The micrographs of 30 vol. % solids sintered samples can be visualized in Fig. 10. The images show the grains morphology and the presence of some pores, both in the contour regions and inside the grains. These pores may be related to air entrapment during bodies conformation, as well as to the dextrin burning out in sintering process [44, 64]. The sample containing 1 wt. % dextrin exhibited a non-homogeneous microstructure. By increasing dextrin content, there is a slight decrease in the grain size and an increase in the number of junction points between particles [20]. Microstructure of samples with optimum dispersant content should exhibit a homogeneous distribution and a uniform particle packing [10, 70]. Although the highest degree of densification was observed for the sample containing 1 wt.% dextrin, some isolated closed pores were present in the sintered material [63]. An irregular

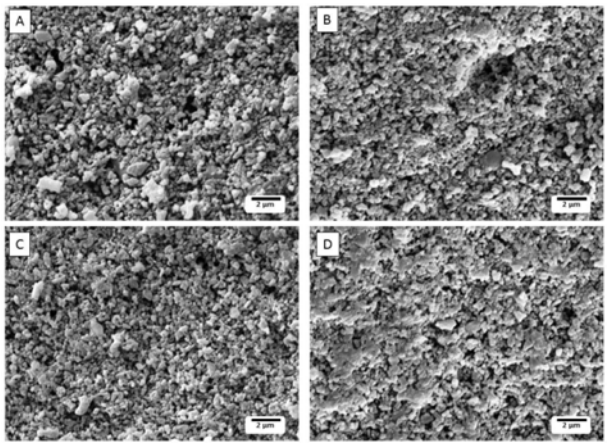

Fig. 12. SEM (5000x) of the sintered samples containing 40 vol.% solids and 0 wt.% (A), 1 wt.% (B), 2.5 wt.% (C) and 5 wt.% (D) dextrin

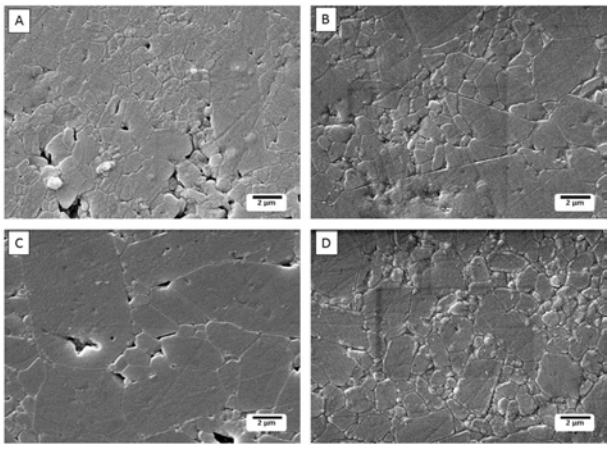

Fig. 13. SEM (5000x) of the sintered samples containing 40 vol.% solids and 0 wt.% (A), 1 wt.% (B), 2.5 wt.% (C) and 5 wt.% (D) dextrin.

granular growth and an increase in the grain boundary adjacent porosity can observed for the sample containing 2.5 wt. % dextrin.

Figs. 11 and 12 show the micrographs of the pre-sintered samples containing 40 vol. % solids and 0, 1, 2.5 and 5 wt. % dextrin. The increase in the suspension solids content contributed to the reduction of bubbles (Fig. 11). The microstructure of these samples also reveals the presence of some agglomerates (Fig. 12). After sintering, the presence of interstitial pores verified for all samples, regardless of the dextrin amount incorporated (Fig. 13). The sample containing 2.5 wt. % of dextrin presented the most compact and uniform microstructure, confirming the densification results. Samples containing 1 wt. % and 5 wt% dextrin exhibited irregular granular growth with varying grain formats.

Conclusions

Dextrin molecules introduced to aqueous alumina suspensions to function as dispersing agents and prevent agglomeration of ceramic particles. The suspensions behavior was pH-dependent, being highly unstable in the presence of dextrin at pHs 8-10. The pH 6 was the best condition for obtaining compact pure Al_2O_3 systems. For pH values different from 6, agglomerated Al_2O_3 particles formed larger sedimentation heights and clarified supernatants. The saturation of the Al_2O_3 active sites occurred through the formation of a dextrin-adsorbed monolayer at an additive concentration of 1.5 wt. %. At this first adsorbed monolayer, the extent of the acid-base interaction between alumina and dextrin will determine whether the adsorption mechanism is through hydrogen bonding or via chemical complexation. For dextrin contents higher than 1.5 wt. %, the results indicated the formation of a second adsorption layer, probably related to dextrin-dextrin interactions. The presence of dextrin also influenced the microstructure and density of the ceramic specimens. The highest percentage of densification was 96.25% (in relation to the alumina theoretical density) for the sample containing 30 vol. % solids and 1 wt. % dextrin. The samples densities directly affected by the presence of entrapped air bubbles in the compacted structure. By increasing dextrin content, there were a slight decrease in the grain size and an increase in the number of junction points between particles. After sintering, the presence of interstitial pores verified for all samples, regardless of the dextrin amount incorporated. At low dosages, dextrin proved to be efficient in preventing agglomeration of particles, thus providing a better dispersion of aqueous alumina suspensions.

Acknowledgments

The authors thank FAPERGS for a scholarship to Matias Scherer Lunkes. The authors thank also the Prof. Dr. Otávio Bianchi and Prof. Dr. Robinson D. Cruz for the contributions and suggestions.

References

1. J.S. Reed, in “Principles of Ceramics Processing” (Wiley,1995) p.688.
2. J.A. Lewis, JACS 83[10] (2000) 2341-2359.
3. C. Xiao, H. Chen, X. Yu, L. Gao and L. Guo, JACS 94[10] (2011) 3276-3281.
4. M. Azar, P. Palmero, M. Lombardi, V. Garnier, L. Montanaro, G. Fantozzi and J. Chevalier, JECS 28[6] (2008) 1121-1128.
5. P.C. Hidber, T.J. Graule and L.J. Gauckler, JACS 79[7] (1996)1857-1867.
6. P. Falkowski, P. Bednarek, A. Danelska, T. Mizerski and M. Szafran, JECS 30[14] (2010) 2805-2811.
7. K. Sato, H. Yilmaz, A. Ijuin, Y. Hotta and K. Watari, Appl. Surf. Sci. 258[8] (2012) 4011-4015.
8. C.H. Schilling, M. Sikora, P. Tomasik, C. Li and V. Garcia, JECS 22[6] (2002) 917-921.
9. S. Çinar and M. Akinc, JECS 34[8] (2014) 1997-2004.
10. A. Kumar, K. Mohanta and D.P. Kumar, Ceram. Int. 40[4] (2014) 6271-6277.

11. P.S. Bhosale and J.C. Berg, Colloid Surface A 362[1-3] (2010) 71-76.
12. H. Gocmez, Ceram. Int. 32[5] (2006) 521-525.
13. P. Somasundaran, X. Yu and S. Krishnakumar, Colloid Surface A 133[1-2] (1998) 125-133.
14. J.J. Gulicovski, L.S. Cerovic, S.K. Milonjic and I.G. Popovic, J. Serb. Chem. Soc. 73[8-9] (2008) 825-834.
15. M. Szafran and G. Rokicki, AST 45[1] (2006) 453-461.
16. M. Rahaman, in "Ceramic Processing" (Taylor & Francis Group, 2006) p.473.
17. M. Sikora, C.H. Schilling and P.L. Tomasikc, JECS 22[5] (2002) 625-628.
18. J. Webber, J.E. Zorzi, C.A. Perottoni, S. Moura e Silva and R.C.D. Cruz, JMatS 51[11] (2016) 5170-5184.
19. C.H. Schilling, R.A. Bellman, R.M. Smith and H. Goel, JACS 82[1] (1999) 57-66.
20. A.S.-M. Safinajafabadi, R.; Karimi, Z., Mater. Res. Bull. 47[12] (2012) 4210-4215.
21. A. Beaussart, A.M. Mierczynska-Vasilev, S.L. Harmer and D.A. Beattie, J. Colloid Interface Sci. 357[2] (2011) 510-520.
22. Q. Liu, Y. Zhang and J.S. Laskowski, Int. J. Miner. Process. 60[3-4] (2000) 229-245.
23. P. Tomasik, C.H. Schilling, R. Jankowiak and J.-C. Kim, JECS 23[6] (2003) 913-919.
24. P. Tomasik, M. Pałasiński and S. Wiejak, Adv. Carbohydr. Chem. Biochem. 47[1] (1989) 203-278.
25. B.M. Cerrutti, C.S. Souza, A. Castellan, R. Ruggiero and E. Frollini, Ind. Crops Prod. 36[1] (2012) 108-115.
26. A.U. Khan, B.J. Briscoe and P.F. Luckham, Colloid Surface A 161[2] (2000) 243-257.
27. M. Montero, T. Molina, M. Szafran, R. Moreno and M.I. Nieto, Ceram. Int. 38[4] (2012) 2779-2784.
28. M.R.B. Romdhane, S. Baklouti, J. Bouaziza, T. Chartier, J-F. Baumard, JECS 24[9] (2004) 2723-2731.
29. P. Bednarek, M. Szafran and T. Mizerski, AIST 62[1](2010)169-174.
30. Y. Fukuda, T. Togahi, Y. Suzuki, M. Naito, H. Kamiya, Chem. Eng. Sci. 56[9] (2001) 3005-3010.
31. S. Lofty, Int. J. Biol. Macromol. 44[1] (2009) 57-63.
32. M. Dal Bó, W.F. Neves and S. Amaral, Cerâm. Industr. 7[2] (2002) 42-46.
33. ASTM, in "Standard Test Method for Water Absorption, Bulk Density, Apparent Porosity, and Apparent Specific Gravity of Fired Whiteware Products" (West Conshohocken, 2006) p.3.
34. J. Catafesta, R. Andreola, C.A. Perottoni and J.E. Zorzi, Cerâm. 53[325](2007)29-34.
35. A.A. Parker, M.-Y. Tsai, G. Biresaw, T.T. Stanzione, G.H. Armstrong and J.J. Marcinko, in "Settling behaviour of alumina dispersions and resultant green body characteristics: solvent, binder and dispersant competition in model systems "(Cambridge University Press,1992) p.273.
36. L.B. Palhares, C.G. Santos and T.N. Hunter, Int. J. Miner. Process. 150[1] (2016) 39-46.
37. A.M. Raichur, J. Dispersion Sci. Technol. 28[8] (2007) 1272-1277.
38. Q. Liu, J.S. Laskowski,, J. Colloid Interface Sci. 130[1] (1989) 101-111.
39. Q. Liu, J.S. Laskowski, Int. J. Miner. Process. 26[3-4] (1989) 297-316.
40. Y. Chen, S. Liu and G. Wang, J. Colloid Interface Sci. 303[2] (2006) 380-387.
41. X. Ma, M. Pawlik, J. Colloid Interface Sci. 313[2] (2007) 440-448.
42. M. Wiśniewska, K. Terpiłowski, S. Chibowski, T. Urban, V.I. Zarko and V.M. Gun'ko, Int. J. Miner. Process. 132[1] (2014) 34-42.
43. D.-M. Liu, Ceram. Int. 26[3] (2000) 279-287.
44. S. Mohanty, B. Das and S. Dhara, JAsCerS 1[2] (2013) 184-190.
45. G.B. Raju, A. Holmgren and W. Forsling, J. Colloid Interface Sci. 193[2] (1997) 215-222.
46. N. Pellerin, J.T. Staley, T. Ren, G.L. Graff, D.R. Treadwell and I.A. Aksay, Mater. Res. Symp. Soc. 218[1] (1991) 123-128.
47. G. Bertranda, C. Filiatreb, H. Mahdjouba, A. Foissyb, C. Coddet, JECS 23[2] (2003) 263-271.
48. S. Manjula, S.M. Kumar, A.M. Raichur, G.M. Madhu, R. Suresh, M.A.L.A. Raj, Cerâm. 51[318] (2005) 121-127.
49. C.H. Schilling, S.B. Biner, H. Goel, J. Jane, J. Environ. Polym. Degrad. 3[3] (1995) 153-160.
50. B.P. Singh, S. Bhattacharjee, L. Besra and D.K. Sengupta, Ceram. Int. 30[6] (2004) 939-946.
51. W.J. Tseng and K.-H. Teng, MSE:A 318[1-2] (2001) 102-110.
52. Y. Liu, L. Gao, J. Guo, Colloid Surface A 174[3] (2000) 349-356.
53. L. Jiang, L. Gao, Mater. Chem. Phys. 80[1] (2003) 157-161.
54. M.S. Lim, K. Feng, X. Chen, N. Wu, A. Raman, J. Nightingale, E.S. Gawalt, D. Korakakis, L.A. Hornak and A.T. Timperman, Langmuir 23[5] (2007) 2444-2452.
55. S.M. Olhero, G. Tarı, M.A. Coimbra and J.M.F. Ferreira, JECS 20[423-429] (2000) 423.
56. E. Grządka, Colloid Surface A 481[1] (2015) 261-268.
57. J.C. Kim, K.H. Auh and C.H. Schilling, Mater. Lett. 40[2] (1999) 209-212.
58. Q. Liu, J.S. Laskowski, Y. Li and D. Wang, Int. J. Miner. Process. 42[3-4] (1994) 251-266.
59. Y. Wang, L. Lin, B.S. Zhu, Y.X. Zhu and Y.C. Xie, Appl. Surf. Sci. 254[20] (2008) 6560-6567.
60. C.H. Schilling, C. Li, P. Tomasik and J.-C. Kima, JECS 22[6] (2002) 923-931.
61. S.R. Sangawar and H.H. Kumar, Def Sci J 56[2] (2006) 269-278.
62. M. Michálková, K. Ghillányová and D. Galusek, Ceram. Int. 36[1] (2010) 385-390.
63. S. Ananthakumar, A.R.R. Menon, K. Prabhakaran and K.G.K. Warrier, Ceram.Int. 27[2] (2001) 231-237.
64. P.A. Ourique, A. Susin Neto, S.G. Echeverrigaray, R.C.D. Cruz and J.E. Zorzi, Cerâm. 59[349] (2013) 71-77.
65. K. Ghillányová, D. Galusek, M. Pentrák, J. Madejová, I. Bertóti, J. Szépvölgyi and P. Šajgalík, Powder Technol. 214[3] (2011) 313-321.
66. B.S.M. Seeber, U.T. Gonzenbach, L.J. Gauckler, J. Mater. Res. 28[17] (2013) 2281-2287.
67. H.N. Yoshimura, A.L. Molisani, G.R. Siqueira, A.C. Camargo, N.E. Narita, P.F. Cesar, H. Goldenstein, Cerâm. 51[319] (2005) 239-251.
68. J.-Z. Li, T. Wu, Z.-Y. Yu, L. Zhang, G.-Q. Chen and D.-M. Guo, J. Mater. Process. Technol. 212[3] (2012) 571-579.
69. Y. Jia, Y. Kanno and Z.-P. Xie, JECS 22[12] (2002) 1911-1916.
70. A. Lasalle, C. Guizard and S. Deville, J. Am. Ceram. Soc. 94[1] (2011) 244-249.